The 2016 World Congress on
The 2016 Structures Congress (Structures16)
Jeju Island, Korea, August 28-September 1, 2016

Development of a Structural Health Monitoring System Based on Multifractal Detrended Cross-Correlation Analysis

*Tzu-Kang Lin[1)] and Yi-Hsiu Chien[2)]

[1), 2)] Department of Civil Engineering, NCTU, East Dist. 300, Taiwan
[1)] tklin@nctu.edu.tw

ABSTRACT

In recent years, multifractal-based analyses have been widely applied in engineering. Among these methods, multifractal detrended cross-correlation analysis (MFDXA),a branch of fractal analysis, has been successfully applied to finance and biomedicine. As only few researches have been devonted in civil engineering, a structural health monitoring (SHM) system based on MFDXA is proposed in this study. By measuring the ambient vibration signal from a structure, parameters including the q^{th} order detrended covariance, the q-order Hurst exponent, and the q-order singularity dimension are adopted for damage assessment. Among the proposed algorithm, the damage condition is first distinguished by multifractal detrended fluctuation analysis (MFDFA). The relation between the q^{th} order detrended covariance, the length of segment and q order is further explored. By visualizing the dissimilarity between the damage and undamaged cases on the contour diagram, the damage location can be detected by the signals measured from different floors. Moreover, a damage index is proposed to efficiently simplify and enhance the SHM process. In order to demonstrate the performance of the proposed SHM algorithm, a seven-story benchmark structure at National Center for Research on Earthquake Engineering (NCREE) is employed for experiment verification. Based on the results, the damage condition and orientation can be correctly identified by the MFDXA algorithm and the proposed damage index. As only the ambient vibration signal is required with a set of initial reference measurement, the proposed structure health monitoring system can provide a low-cost, efficient, and reliable monitoring method than the conventional SHM methods.

[1)] Associate Professor

[2)] Graduate Student

1. Introduction

In developed and economically advanced countries, how to prevent the huge loss of human life and property has become a global issue. Structure health monitoring is aimed to diagnose the damage condition and specify the damage location. There are two main categories in SHM determining the degree of structural damage, global and local health monitoring. The first type is the global health monitoring method, which is used to detect the information from entire structure and reflect the characteristics of damaged condition by the change of global dynamic properties of structure such as damping ratio, mode shape, frequency. Several examples of well-known techniques are natural frequency-based method(Fan 2011), mode shape curvature-based method(Pandey 1991), and mode shape-based method(Farrar 1997).

The second type is the local health monitoring method, which is utilized to observe the behavior of potential damage locations or critical areas and to track the size of damage. A number of techniques are developed for damage location diagnosis which is based on few simple concept such as visual inspection(Aktan 2003), strain, and displacement(Jang 2007). Although global health monitoring techniques are able to access the existence of damage, the location of damage and quantification of the severity of damage are relatively difficult. Moreover, time consuming, high cost, and accuracy are tough problem that make local health monitoring techniques more difficult to be worked on than global health monitoring. In current researches, the combination of both methods are essential for SHM.

In 1983, Mandelbrot studied the shape of nature and discovered the fractal phenomena.(Mandelbrot 1983) The contour of rock or other nature things shows the similarity in different scales. The scaling behavior of fractal theory is able to interpret the complex, irregular, non-stationary, and fragmented change in shape and time series.(Kantelhardt 2008; Peng 1995) Many algorithms were developed to describle the scaling behavior base on fractal thoery and compared their advantages and limits.

Multifractal detrended fluctuation analysis(MFDFA), a generalization of detrended fluctuation analysis(DFA)(Peng 1995)which is based on fractal theory, was proposed by Kantelhardt in 2002.(Kantelhardt 2002) Firstly, in 1999, Ivanov studied the multifractality in a biological dynamical system, the human heartbeat. The study uncovered a loss of multifractality for a life-threatening condition,congestive heart failure, demonstrating an explicit relation between the nonlinear features.(Ivanov 1999) 2012, Ihlen introduced MFDFA into MATLAB code for estimating the multifractal spectrum of biomedical time series. The multifractal spectrum reflects the variation in the fractal structure of the biomedical time series and identifies the pathological conditions. (Ihlen 2012) Besides that, Srimonti used MFDFA to study the human gait time series for normal, Parkinson’s disease, and Huntington’s disease. This study reveals that long range correlation is responsible for multifractality and the degree of multifractality of normal set is bigger than diseased set. The MFDFA method is capable of distinguishing between normal and diseased set, however, when it comes to two types diseased set, the MFDFA method does not work.(Dutta 2013) In recent, Haris applied MFDFA to animal vocalizaions, seahorse feeding clicks, for comparing the seahorse body sex, size, and weight. This work underscores the versatility of the MFDFA to investigate bioacoustics observations and the nonliearities. (Haris 2014) In many present studies validate the multifractal

properities of natural things by MFDFA, however, it is not sufficient to determine the details of different sets.

In 2008, Zhou proposed a method called multifractal detrended cross-correlation analysis(MFDXA), which is based on detrended covariance to investigate the multifractal behaviors between two time series or high-dimensional quantities. Zhou apply the MFDXA to the daily closing prices of Dow Jones Industrial Average and National of Securities Dealers Automated Quotation indices, showing power-law dependence for positive q order.(Zhou 2008) In earthquake engineering, Shadkhoo use MFDXA to investigate the cross-correlation of temporal and spatial inter-events seismic data. The results shows that the inter-events of temporal and spatial seismic series exist weak multifractality in spite of the strong multifractal behavior of temporal and spatial time series, separately.(Shadkhoo 2009) In financial field, He applies MFDXA to investigate the cross-correlation of agricultural futures markets in two highly correlated economies, China and USA. The study validates the strong cross-corralation of China's and US agricultural futures markets and share the similar multifractal structure.(He 2011) Also, Wang find that the price and the load time series in California power market and JPM power market exhibit long-term correlation. However, the cross-correlation is weaker in the California market than in the JPM market. In biomedical field, Ghosh use MFDXA to study the EEG data of epileptic patients in 2014.This study reveals the degree of cross-correlation is more among seizure and seizure free interval in epileptogenic zone, indicating that these data are significant for diagnosis.(Ghosh 2014) Recently, Dutta studies the human gait pattern of normal people and patients who suffering from Parkinson's disease. It reveals that the degree of multifractality and the degree of correlation are greater for normal set than diseased set, besides, it also verifies that the results of MFDFA method are not sufficient to distinguish between normal and disesed set.(Dutta 2016)

In the last decades, MFDFA and MFDXA have the outstanding finding in different fields, especially biomedical, economics, and finance. This main goal of this study is to utilize the advantages of MFDFA and MFDXA for damage condition and location detection. MFDFA is introduced to determine damage condition in the structure by measuring the dynamic signal from a single sensor which is set on each floor. Meanwhile, MFDXA is for the purpose of locating the damaged floor of the structure. The flowchart of the proposed SHM system is shown in Fig. 1.

The remainder of this paper is organized as follows. First, the basic concept of MFDFA, MFDXA, and the proposed damage index are describled. Moreover, the practial experimental verification is conducted by using seven-story steel benchmark structure located at National Center for Research on Earthquake Engineering(NCREE). Based on experimental results, the damage condition and location can be assessed. Finally, a summary is given and conclusions are drawn.

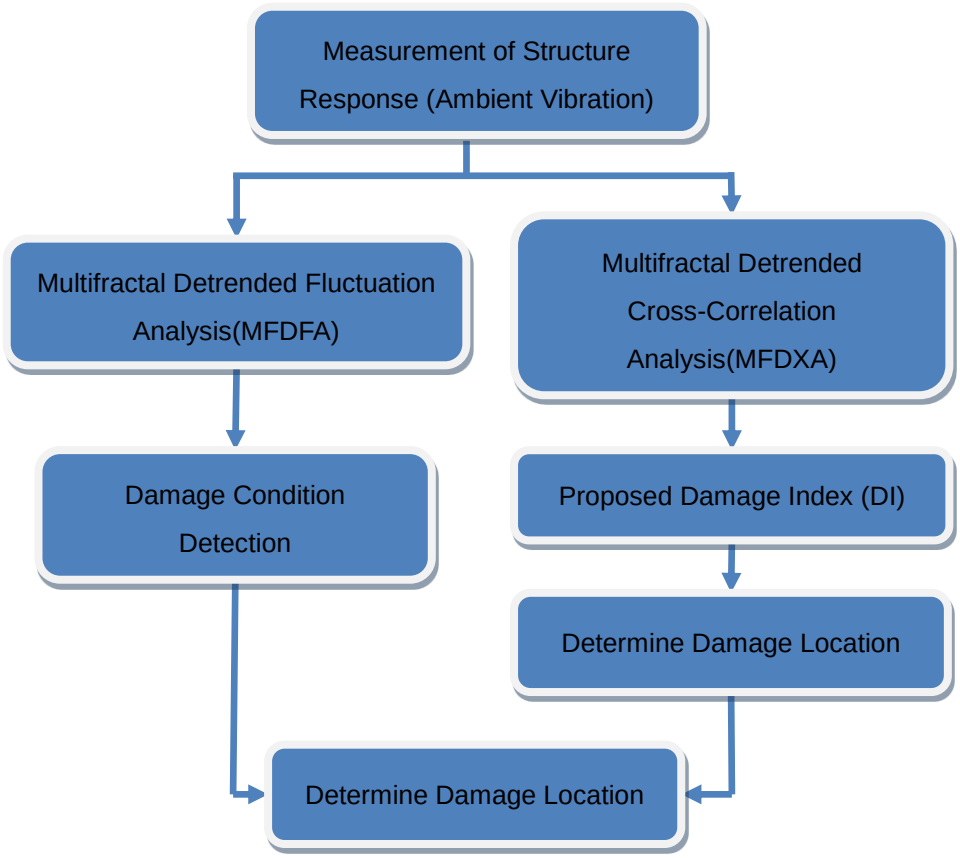

Fig. 1 Flowchart of proposed SHM system

2. The proposed SHM method

2.1 Multifractal detrended fluctuation analysis(MFDFA)

The MFDFA method is a generalized multifractal DFA. A brief theoretical overview is summarize in this section(Kantelhardt 2002; Ihlen 2012). For a time series of finite length N, the first step involves the subtraction of the mean X_{ave} from the vibration time series $X(i)$.

$$X_{ave} = \frac{1}{N}\sum_{i=1}^{N} X(i) \tag{1}$$

$$Y(i) \equiv \sum_{k=1}^{i}[X(k) - X_{ave}] \quad \text{for } i=1...N \tag{2}$$

$Y(i)$ is defined as the cumulated data series, which is divided into N_s non-overlapping bins of equal length s, $N_s = \text{int}(N/s)$. To avoid omitting the short segment at the end of the profile, the same process is repeated from the opposite end of the time series. Hence, $2N_s$ bins are obtained and the local linear trend for each bin is calculated by a least-square fitting for each segment v. Furthermore, the variance is calculated by

$$F^2(s,v) = \frac{1}{s}\sum_{i=1}^{s}\{Y[(v-1)s+i] - y_v(i)\}^2 \tag{3}$$

for each segment v, $v = N_s + 1,...2N_s$

$$F^2(s,v) = \frac{1}{s}\sum_{i=1}^{s}\{Y[N-(v-N_s)s+i] - y_v(i)\}^2 \tag{4}$$

$y_v(i)$ is the linear fitting polynomial in the segment v. Finally, for each of the $2N_s$ segments, the q-order fluctuation function is obtained.

$$F_q(s) = \left\{\frac{1}{2N_s}\sum_{v=1}^{2Ns}\left[F^2(s,v)\right]^{\frac{q}{2}}\right\}^{\frac{1}{q}} \tag{5}$$

In general, *q* can be any real value except zero. for *q*=0

$$F_0(s) \equiv \exp\left\{\frac{1}{4N_s}\sum_{v=1}^{2Ns}\ln\left[F^2(s,v)\right]\right\} \tag{6}$$

The scaling behavior of the fluctuation function is determined by analyzing the slope of the log-log plots $F_q(s)$ versus *s* for different *q*. If the series $x(i)$ have long-range power-law correlation, $F_q(s)$ with *s* is described as

$$F_q(s) \propto s^{H(q)} \tag{7}$$

H(q) is the slope and be termed as generalized *q* order Hurst exponent. For stationary time series, when *q* is equal to 2, *H(2)* is identical with the Hurst exponent. A monofractal time series is independent of *q*, remaining the unique *H(q).* The positive and negative values of *q* describes the scaling behaviors with large and small fluctuations, respectively.

The *H(q)* is directly related to the classical scaling exponent *τ(q)*. The relation between *H(q)* and *t(q)* can be represented as

$$\tau(q) = q \times H(q) - 1 \tag{8}$$

Another way to characterize a multifractal series is the singularity spectrum, also called q-order singularity dimension *Dq*, which is related to τ(q) via a Legendre transform.(Ihlen 2012; Kantelhardt 2002).

$$hq = \tau'(q) = H(q) + q \times H'(q) \tag{9}$$

$$Dq = q \times hq - \tau(q) = q\left[hq - H(q)\right] + 1 \tag{10}$$

where *hq* is singularity exponent or strength and *Dq* shows the dimension of the subset of the series.

For N-floor structural dynamic time series with different time scale, MFDFA can verify the existing multifractal properties; however, MFDFA does not consider the influence of signal from the different floor. In summary, MFDFA is not a powerful tool to determine the damage location.

2.2 Multifractal detrended cross-correlation analysis(MFDXA)

In order to study the degree of correlation between two nonstationary time series, MFDXA is adopted. Consider two time series Xi and Yi of length *N*, with *i* = 1,2..,*N.* Then an accumulated deviation series are formed by subtracting the mean values X_{ave}

and Y_{ave} from the respective time series.

$$X(i) \equiv \sum_{k=1}^{i} [X(k) - X_{ave}] \tag{11}$$

$$Y(i) \equiv \sum_{k=1}^{i} [Y(k) - Y_{ave}] \tag{12}$$

The integration can reduce the level of measurement noise present in experimental data. Each of the accumulated series is divided to N_s non-overlapping bins of equal length s, $N_s = \text{int}(N/s)$. According to the step of the MFDFA procedure, $2N_s$ segments are obtained.

$$F(s,v) = \frac{1}{s}\sum_{i=1}^{s}\{Y[(v-1)s+i] - y_v(i)\} \times \{X[(v-1)s+i] - x_v(i)\}$$

for each segment v, $v = N_s + 1, ...2N_s$

$$F(s,v) = \frac{1}{s}\sum_{i=1}^{s}\{Y[N-(v-N_s)s+i] - y_v(i)\} \times \{X[N-(v-N_s)s+i] - x_v(i)\}$$

$x_v(i)$ and $y_v(i)$ are the fitting polynomials in the segment v. Then the q order detrended covariance $F_q(s)$ is obtained after averaging $2N_s$ bins.

$$F_q(s) = \left\{ \frac{1}{2N_s} \sum_{v=1}^{2Ns} [F(s,v)]^{q/2} \right\}^{1/q} \tag{13}$$

When q is equal to zero, F_q is infinite. A logarithmic averaging procedure is applied as follows.

$$F_0(s) \equiv \exp\left\{ \frac{1}{4N_s} \sum_{v=1}^{2Ns} \ln[F(s,v)] \right\} \tag{14}$$

The procedure is repeated by varying the value of s. $F_q(s)$ increases with increase of the value of *s.* If the series have long-range power-law correlation, then $F_q(s)$ will show power law behavior.

$$F_q(s) \propto s^{\lambda(q)} \tag{15}$$

Scaling exponent $\lambda(q)$ represents the degree of the cross-correlation between the two series. In general $\lambda(q)$ depends on q in multifractal series, on the contrary, $\lambda(q)$ independs on q in monofractal series.

For positive q, $\lambda(q)$ describes the scaling behaviors of the segments with large fluctuations and for negative q, $\lambda(q)$ describes the scaling behaviors of the segments with small fluctuations. The value of $\lambda(q)$=0.5 means the absence of cross-correlation. $\lambda(q)$>0.5 indicates persistent long range cross-correlations while a large value in one variable is likely to be followed by a large value in another variable, while $\lambda(q)$<0.5 indicates anti-persistent cross-correlations while a large value in one variable is likely to be followed by a small value in another variable.(Sadegh Movahed 2008)

2.3 The Proposed Damage Index

In order to improve the accuracy of the SHM system to diagnose the damage location in the structure, a damage index is proposed. By setting the detrended

covariance of healthy case as the reference value, the detrended covariance for different *q*-order and scale is processed to obtain damage index.

In this study, the signal which is measured from the ground floor is cross-correlated with the other floors. For the structure with *X* floor, a total of *X+1* MFDXA curved surface are derived, G*G, G*1F, G*2F,..., G*NF. The undamaged and damaged conditions are expressed respectively as

$$F_q(s)Damage = \{D_1, D_2, D_3, \ldots, D_N\}^T \tag{16}$$

$$F_q(s)Undamaged = \{U_1, U_2, U_3, \ldots, U_N\}^T \tag{17}$$

The symbol D_1 represents the G*G surface for damaged structure. Similarly, symbol U_1 represents G*G surface for undamaged structure. In order to clarify the change between each cross-correlated surface in one damage case, the difference of adjacent floors is calculated, and the damaged case and undamaged case can be expressed respectively as follows:

$$FD = \left\{\sum(D_2 - D_1), \sum(D_3 - D_2), \ldots, \sum(D_N - D_{N-1})\right\}^T \tag{18}$$

$$FU = \left\{\sum(U_2 - U_1), \sum(U_3 - U_2), \ldots, \sum(U_N - U_{N-1})\right\}^T \tag{19}$$

After FD and FU are derived, the proposed damage index for specific floor can be expressed as

$$DI_i = \{FU_i\} - \{FD_i\} \tag{20}$$

where i is the floor number. A negative damage index value indicates the existence of damage on the floor.

As negative *q* tends to reflect the behavior of small fluctuations which is influenced easily by ambient interference, q=1-5 are considered for damage index diagnosis in this study. Moreover, because of instability of the ambient vibration signal, the covariance F_q is normalized to prevent extreme values which influence the accuracy of damage index.

3. Description of experimental data

In order to verify the practicality of the proposed SHM system, a seven-story benchmark structure at National Center for Earthquake Engineering(NCREE) is employed for experimental verification. Totally 8 sensors are mounted on the benchmark structure and ground to measure the ambient vibration signal.

The dimensions of scale-down steel specimen are shown in Fig. 2a. The height, length, and width of each story are 1.1 m, 1.5 m, and 1.1 m, respectively. The adopted bracing is shown in Fig. 2b, where the cross section is L-shaped steel angles of 65x65x6 (mm). An additional mass of 500 kg was putted on each story to mimic the actual structural characteristics. A velocity meter VSC-15D manufactured by Tokyo Sokushin Co., Ltd was chosen in the experiment and installed in the center of each floor for data acquisition. The layout of a single floor is shown in Fig. 2c.

The damage in this study was simulated by removing the two installed bracing in weak axis direction for every story. The removal of bracing indicated the change of the stiffness on the structural at certain story as the cause of potential damage. Fig. 3d and 3e shows the detail bracing of the experiment. To avoid possible noise during the test, the experiment was conducted at night. The data were recorded for six categories and

sixteen cases at sampling rate 200 Hz in the longitudinal direction. A total of 20 minutes which was divided into four sections was recorded, and each section was treated as a single run of a specific damage condition. Detail of damage in six categories and sixteen cases are listed in Table 1.

(a) Experimental specimen

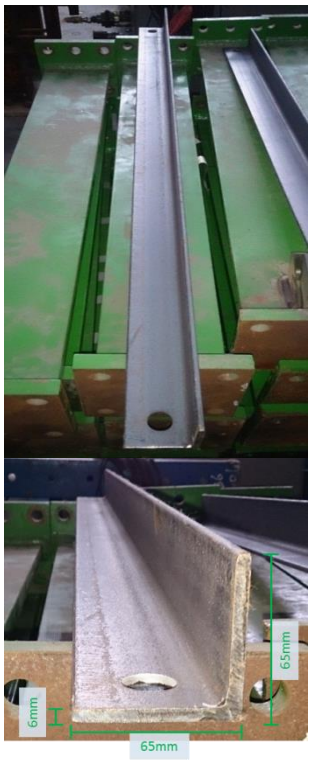

(b) Side view and cross section of bracing

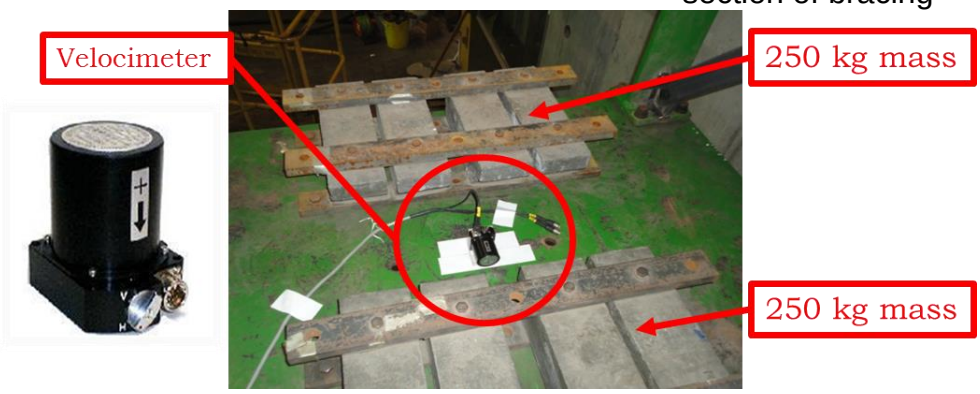

(c) Velocity meter and mass block of a single floor

(d)braced

(e)without bracing

Fig. 2 Layout of experimental structure

Table 1 Total damage cases and category

Damage case	Damage Category	Damage Floors
1	Undamaged	None
2	Slight damage	1F
3		2F
4		3F
5		4F
6		5F
7		6F
8		7F
9	Moderate-damage	1 & 2F
10		3 & 4F
11		5 & 6F
12	Severe-damage	1 & 2 & 3F
13		4 & 5 & 6F
14	Ultimate damage	1 & 2 & 3 & 4F
15		4 & 5 & 6 & 7 F
16	All damage	1-7F

4. Results and discussion

4.1 Damage condition (MFDFA)

The Hurst exponent derived through the MFDFA procedure was first used to detect the damage condition of the structure. The minimum and maximum scales were set to 16 and 1024, respectively. The Hurst exponents with different *q* order in one damage case were averaged as overall exponent.

The damage conditions evaluated for the 16 damage cases are presented in Fig. 3. Each damage case contains four 5-min segments which are pointed in the figure, and it

clearly revealed the existence of damage conditions. For instance, the healthy structure had the lowest *H(q)* value, and the presence of damage was represented by an increase in *H(q).* The damage on the first floor (1F), which would directly have a greater contribution to the global potential failure of the structure, was associated with the higher *H(q)* value compared with the second floor (2F). Similar trends could also be observed for the damage conditions, the case with the damage on the first and second floors (12F) demonstrated a significantly higher *H(q)* value than the cases with damage on the third and fourth floors (34F) and the fifth and sixth floors (56F). Only a minor error was observed that the damage on the second floor (2F) had a lower value than that on the third floor (3F). By using *H(q)* as a measurement of damage condition has been demonstrated.

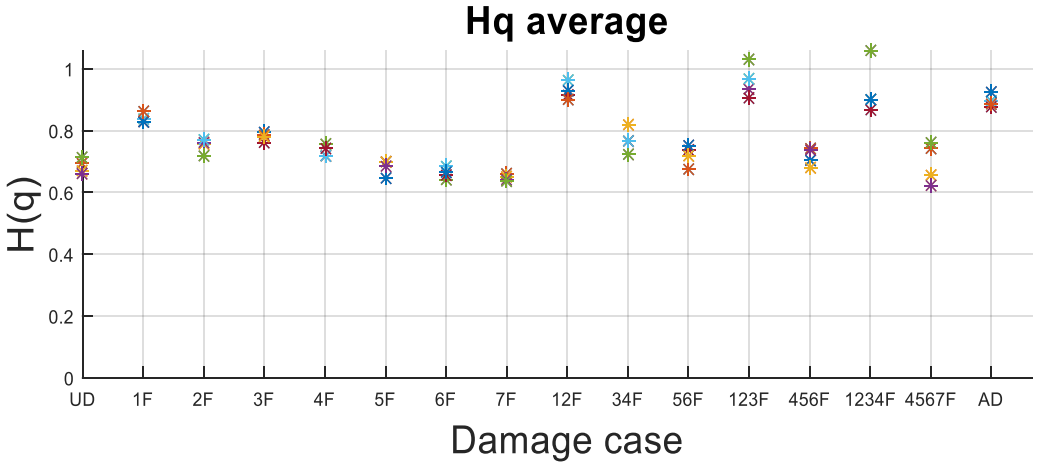

Fig. 3 Distribution of Hurst exponent for different damage cases

4.2 Damage location (MFDXA)

MFDXA was employed to the damage location. From the seven-story structure, eight MFDXA curved surface, namely G*G, G*1F, G*2F,G*3F, G*4F, G*5F, G*6F, and G*7F, were generated through the cross-correlated procedure between the ground and other signals. The healthy structure was analyzed first. The increment between adjacent surfaces, calculated by subtracting the surface of the floor below from the surface of the floor above, was recognized as a reference in the MFDFA as shown in Fig. 4a.

The damage diagnosis result for the first floor (1F) is shown in Fig. 4b. The result clearly revealed that the increment between G*G and G*1F surface jumped suddenly, whereas the other surface were close to each other. Compared with the increment of reference, this trend showed the presence of damage on the first floor. Fig.4c shows the case with the damage on the third and fourth floors (34F). The jump of surfaces of the third and fourth floors indicated that damage occurs on the third and fourth floors.

Similar trends are observed in Fig.4d, the damage from the first to third floor case (123F). The MFDXA surfaces 1F, 2F, and 3F jumped rapidly, forming a massive region between other floors. However, the result of damage from the fourth to seventh floor did not follow this trend, there was a error on the surface 7F which did not form a region between other undamaged floors as shown in Fig. 4e. Also, in all damage case (AD), the seven surfaces did not follow this trend, the increment between adjacent surfaces

did not present a rapid jump like other cases.

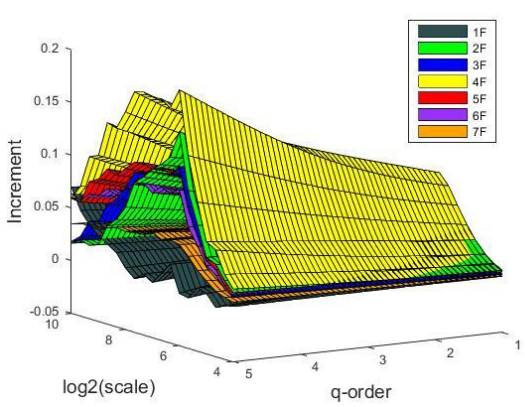

(a) Healthy condition

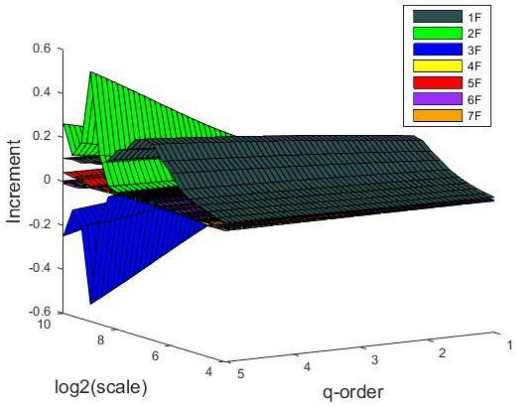

(b) Damage on the first floor

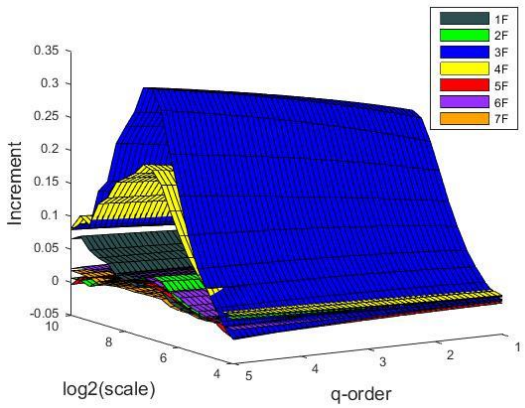

(c) Damage on the third and fourth floor

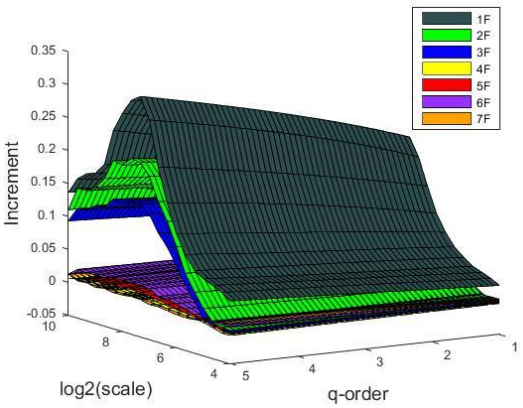

(d) Damage from the first to third floor

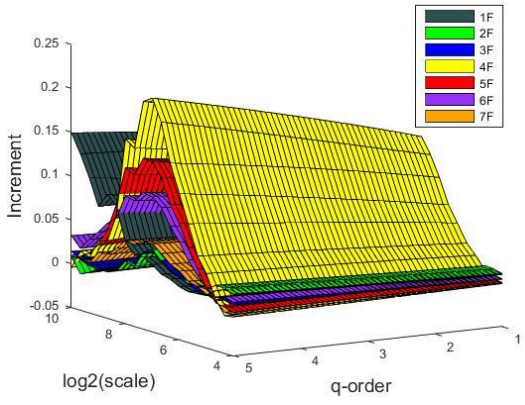

(e) Damage from the fourth to seventh floor

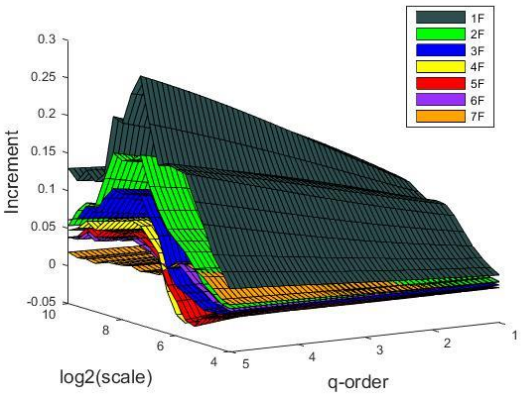

(f) Damage on all floors

Fig. 4 The experimental MFDXA curved surface

4.3 Damage location (Damage Index)

Although most of damage locations could be distinguished by the MFDXA surfaces, the absence of quantization made this method unpersuasive. Therefore, the proposed damage index was employed to improve the reliability and practicability of the SHM system. The damage index values for five selected cases are provided in Fig. 5.

As shown in Fig.5a, negative damage index values occurred clearly on the first floor, and the other index remained positive. The stiffness reduction, which was set by removing the brace on the first floor, caused this phenomenon. Hence, the change on the first floor was different to that in the healthy condition. The damage location could be detected by the damage index.

Similar trend were observed the case of damage on the third and fourth floors, where the proposed damage index accurately detected damage locations (Fig. 5b). Negative values were observed on the third and fourth floors. As expected, the case of damage from the first to third floors was also diagnosed correctly. The damage index values of the damaged floors were negative, whereas the undamaged floors were positive.

Fig. 5d showed the damage index for damage from the fourth to seventh floors. Most of the damaged floors could be detected, only the signal, recorded in the second 5-min section, had an extremely small positive value. However, misjudgment occurred for damage on all floors. The damage index appeared complex manners compared with the former damage cases.

The MFDXA method was compared with other methods in the field of SHM. A total of 15 damage cases were analyzed using the DCCA, damage index based on DCCA, MFDXA, and the proposed damage index, and the results are listed in Table 2. As indicated, the accuracy of DCCA was 75%; the accuracy of DCCA damage index was 87.5%. Nevertheless, the accuracy rate of MDFXA was 80%. Besides, the proposed damage index could improve the accuracy to 93.33%, and only the case of all damage failed. The result shows that a more reliable method for SHM is provided by utilizing the multifractality compared with the DCCA method.

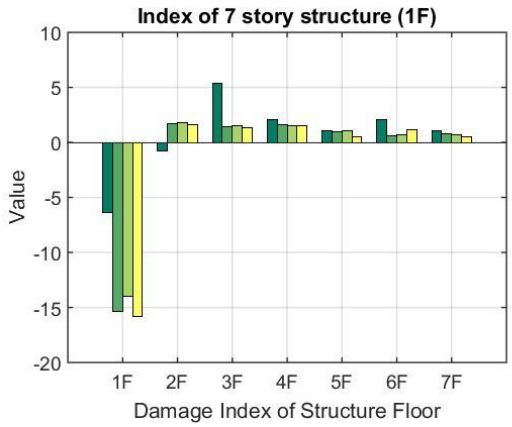

(a) Damage on the first floor

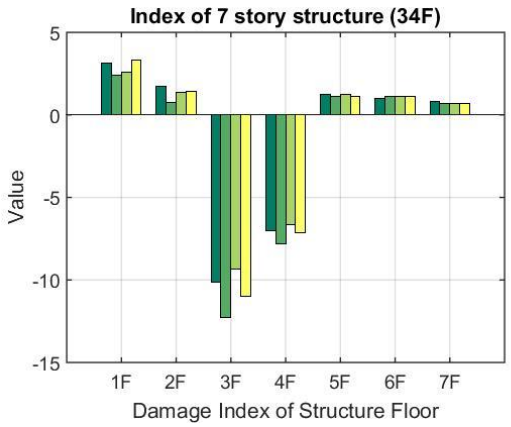

(b) Damage on the third and fourth floor

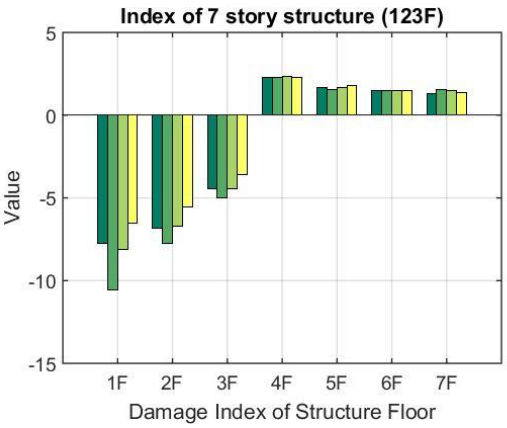

(c) Damage from the first to third floor

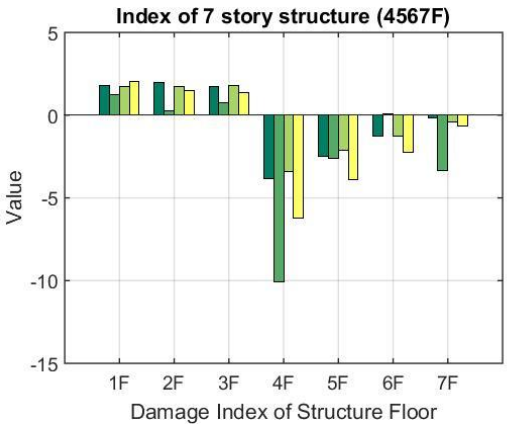

(d) Damage from the fourth to seventh floor

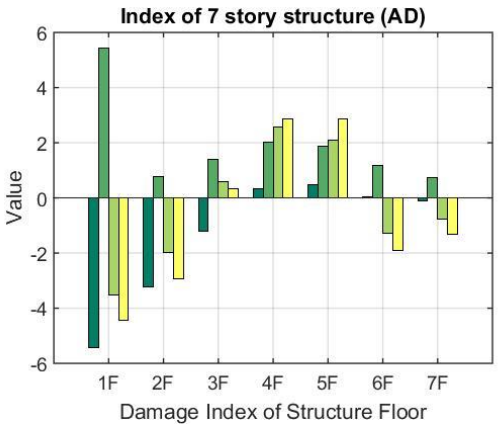

(e) Damage on all floors

Fig.5 The damage index of experimental condition

Table 2 Damage location detection for different methods

Damage Location	Method			
	Detrended Cross-Correlation Analysis (DCCA)	Damage Index (DCCA)	Multifractal Detrended Cross-Correlation Analysis (MFDXA)	Damage Index (MFDXA)
1F	C	C	C	C
2F	C	C	C	C
3F	C	C	C	C
4F	C	C	C	C
5F	C	C	C	C

6F	F(2&6F)	F(5&6F)	C	C
7F	F(1&2&3F)	C	F(7F)	C
1&2F	C	C	C	C
3&4F	C	C	C	C
5&6F	C	C	C	C
1&2&3F	C	C	C	C
4&5&6F	C	C	C	C
1&2&3&4F	C	C	C	C
4&5&6&7F	F(4&5&6F)	C	F(7F)	C
Damaged all	F(1&2&3&4F)	F(2&3&4&7F)	F(all floors)	F(3&4&5&6F)
Accuracy (%)	75%	87.5%	80%	93.33%

C: Correct, F: False

5. Summary and Conclusion

By adopting multifractal analysis, which is capable of interpreting the complex, irregular, and disordered phenomena, a SHM system based on MFDFA and MFDXA is proposed in this study. MFDFA was employed to determine the damage condition of structure. The Hurst exponent value, an important parameter in MFDFA, was used to show the degree of damage. Moreover, MFDXA was used to localize the damage location in the structure. The detrended covariance, derived from the MFDXA algorithm, was utilized to identify the damage location.

An experimental verification was carried out on a seven-story scaled-down benchmark structure at NCREE. Sixteen damage cases were executed and analyzed. On the basis of the MFDFA method, the damage condition could be assessed through *H(q).* Moreover, the damage location could be localized using the MFDXA technique with an accuracy of 80%. Using the proposed damage index further improved the accuracy to 93.33%. As only ambient vibration is required in a set of initial reference measurements, the proposed system offers an easy and alternative strategy for practical SHM.

REFERENCES

Aktan, A. and Catbas, F. (2003), “Development of a model health monitoring guide for major bridges,” *… Dev.*, no. July, pp. 1–290.

Dutta Srimonti, Ghosh Dipak, Chatterjee Sucharita. (2013). "Multifractal detrended fluctuation analysis of human gait diseases," *Frontiers in physiology*,4,1-7.

Dutta Srimoti, Ghosh Dipak, Samanta Shukla. (2016), “Non linear approach to study the dynamics of neurodegenerative diseases by Multifractal Detrended Cross-correlation Analysis- A quantitative assessment on gait disease,” *Physica A*, 488, 181-195.

Fan, W. & Qiao, P. (2011), “Vibration-based Damage Identification Methods : A Review and Comparative Study,” vol. 10, no. 1, pp. 83–111.

Farrar, C.R. and James, G.H. (1997), “System Identification From Ambient Vibration Measurements on a Bridge,” *J. Sound Vib.*, vol. 205, no. 1, pp. 1–18.

Ghosh Dipak, Dutta Srimonti, Chakraborty Sayantan. (2014), “Multifractal detrended cross-correlation analysis for epileptic patient inseizure and seizure free status,” *Chaos, Solitons & Fracatls*, 67, 1-10.

Haris, K., Bishwajit Chakraborty, Menezes, A., Sreepada, R. A., Fernandes, W. A. (2014), “Multifractal detrended fluctuation analysis to characterize phase coupling in seahorses (Hippocampus kuda) feeding clicks,” *Acoustical Society of America*, 136, 1972-1981.

He, L.Y., Chen, S.P. (2011), “Multifractal Detrended Cross-Correlation Analysis of agricultural future markets,” *Chaos, Solitons & Fracatls*, 44, 355-361.

Ihlen, E.A.F. (2012). “Introduction to multifractal detrended fluctuation analysis in Matlab,” *Frontiers in physiology*, 3, 1-18.

Ivanov, P. Ch., Nunes Amaral, L. A., Goldberger, A. L., Havlin, S., Rosenblum, M. G.,Struzik, Z. R., Eugene Stanley, H., (1999). “*Multifractality in human heartbeat dynamics*,” Macmillan Magazines, Ltd, 399, 461-465.

Jang, S.A., Sim, S. and Spencer Jr, B. F. (2007), “Structural Damage Detection Using Static Strain Data,”.

Kantelhardt ,J. W., Zschiegner, S. A., Koscielny-Bunde, E., Havlin, S., Bunde, A., Stanley, H. E., (2002) “Multifractal detrended fluctuation analysis of nonstationary time series,” *Physica A*, 316, 87-144.

Kantelhardt, J.W. (2008), “Fractal and Multifractal Time Series,” pp. 1–59.

Mandelbrot, B.B. (1983), “The Fractal Geometry of Nature,” *American Journal of Physics*, vol. 51, no. 3. p. 286.

Pandey, a.K., Biswas, M. and Samman, M.M. (1991), “Damage detection from changes in curvature mode shapes,” *J. Sound Vib.*, vol. 145, no. 2, pp. 321–332.

Peng, C.K., Havlin, S., Eugene Stanley, H., Goldberger, Ary L., (1995). “Quantification of scaling exponents and crossover phenomena in nonstationary heartbeat time series,” *American Institute of Physics*, Vol. 5, No. 1.

Peng, C.K., Buldyrev, S.V., Goldberger, A.L., Havlin, S., Mantegna, R.N., Simons, M. and Stanley, H.E. (1995), “Statistical properties of DNA sequences,” *Physica A*, vol. 221, pp. 180–192.

Sadegh Movahed, M., Hermanis, E. (2008), “Fractal analysis of river flow fluctuations,” *Physica A*, 387, 915-932.

Shadkhoo, S., Jafari, G. R. (2009), “Multifractal detrended cross-correlation analysis of temporal and spatial seismic data,” *Eur. Phys. J. B* 72,679-683.

Zhou, W.Z. (2008), “Multifractal detrended cross-correlation analysis for two nonstationary signals,” *Physical review*, E77, 066211.